

Frequency, thermal and voltage supercapacitor characterization and modeling

F. Rafik^{a,b}, H. Gualous^{b,*}, R. Gallay^c, A. Crausaz^a, A. Berthon^b

^a Haute Ecole Arc Ingénierie, CH-2400 Le Locle, Switzerland

^b L2ES-UTBM-Université de Franche Comté, Rue Thiery-Mieg, F90010 Belfort, France

^c MAXWELL Technologies, CH-1728 Rossens, Switzerland

Received 10 February 2006; received in revised form 25 November 2006; accepted 1 December 2006

Available online 20 December 2006

Abstract

A simple electrical model has been established to describe supercapacitor behaviour as a function of frequency, voltage and temperature for hybrid vehicle applications. The electrical model consists of 14 RLC elements, which have been determined from experimental data using electrochemical impedance spectroscopy (EIS) applied on a commercial supercapacitor.

The frequency analysis has been extended for the first time to the millihertz range to take into account the leakage current and the charge redistribution on the electrode. Simulation and experimental results of supercapacitor charge and discharge have been compared and analysed. A good correlation between the model and the EIS results has been demonstrated from 1 mHz to 1 kHz, from -20 to 60 °C and from 0 to 2.5 V.

© 2006 Elsevier B.V. All rights reserved.

Keywords: Supercapacitor modeling; Supercapacitor thermal characterization; Supercapacitor dynamic behavior

1. Introduction

The degradation of the air quality due to vehicle gas emissions in big cities has contributed to the need for research of environmentally clean solutions to resolve large transportation energy requirements. Different electrical solutions have been proposed to get a substitution of the internal combustion engine. The full electrical one, mainly based on electrical storage with batteries (Pb, Ni–Cd, MNiH, Li ion, etc.), suffers from very high cost, poor depth of discharge performance and short lifetime. An optimisation of the costs and the performances leads to the study of hybrid solutions incorporating supercapacitors [1]. These latter bring the power capability and the cyclability performance required. The hybrid solution allows either the downsizing of powerful power generator like the internal combustion engine, or the incorporation of a weak power generator such as fuel cell. Supercapacitors provide the power for the vehicle acceleration and they are able to recover and store the braking energy. Studies have shown that operation with supercapacitors may lead to

fuel consumption reduction of 15% in car applications and even 20% in bus applications.

Table 1 presents a comparison between battery, supercapacitor and electrolytic capacitor characteristics. It's clear that the supercapacitor has several advantages compared to the other elements.

The elementary structure of a supercapacitor includes two electrodes, separated by a porous membrane and impregnated with an organic electrolyte. The electrode is made of an aluminium current collector foil, supporting the activated carbon powder. The separator is inserted between the two electrodes and acts both as an electronic insulator and an ionic conductor. The assembly of the device is achieved by winding the different foils, like in classical capacitors.




The supercapacitor operating principle is based on the double layer at the interface between the activated carbon electrode and the organic electrolyte when a voltage is applied to the terminals. The energy storage for double layer type capacitors is primarily electrostatic, rather than faradaic as is the case for batteries, but likely includes a pseudocapacitive component to contributing to the total capacitance [2].

The supercapacitor capacitance may lie in the range of 1–5000 F. The maximum voltage typically up to 3 V is limited

* Corresponding author.

E-mail address: hamid.gualous@univ-fcomte.fr (H. Gualous).

Table 1
Comparison between battery, supercapacitor and electrolytic capacitor performances

Storage devices characteristics	Battery 	Supercapacitor 	Capacitor 
Charging time	$1 < t < 5$ h	1–30 s	$10^{-3} < t < 10^{-6}$
Discharging time	$t > 0.3$ h	1–30 s	$10^{-3} < t < 10^{-6}$
Energy density (W h/kg)	10–100	1–10	<0.1
Lifetime (cycle number)	1000	10^6	10^6
Power density (W/kg)	<1000	10,000	>1,000,000
Charge/discharge efficiency	0.7–0.85	0.85–0.98	>0.95

by the decomposition voltage of the electrolyte, mainly because of the presence of impurities.

Considering the physical phenomena in the double layer interface, the supercapacitor cannot be represented by a simple capacitor model formed only by a capacitance, a series and a parallel resistance. The Helmholtz theory permits to explain the different physical phenomenon that happens in the interface between a liquid ionic conductor (electrolyte) and a solid electronic conductor (electrode). The interface is modeled by two superficial distributions of charges, electronic for the electrode, and ionic of opposed sign for the electrolyte.

Several authors propose electric models that describe the electric behaviour of a supercapacitor with a good approximation. Some do not take into account their dynamic behaviour. Others are based on variable time constant models such as the transmission line model [3–5]. The inconvenience of these models is the complex determination of the different elements and the simulation time required which is bound to the RC branch numbers. In this study, an electric model for the Maxwell Technology BCAP0010 supercapacitor is presented. This model takes into account the temperature, voltage and the frequency behaviour. This model is easy to implement in Simplorer or Saber software.

The proposed model is represented in Fig. 1. The originality of this model resides in the limited number of components required to take into account frequency, voltage and temperature dependencies of capacitance, series resistance, redistribution of electrical charges on the electrode surface and leakage current.

2. Electrochemical impedance spectroscopy

Electrochemical impedance spectroscopy (EIS) is used in the characterization of electrochemical behaviour of energy

storage devices. Several authors used this method to characterize electrode materials for supercapacitors, batteries and fuel cells [6,7]. To characterize a supercapacitor, the sweep in frequency must be done for various voltage levels and also for different temperatures. EIS allows the study of the influence of frequency on the electrode series resistance and on specific capacitance.

The measurements have been done on a Maxwell Technologies BCAP0010 supercapacitor, with a nominal capacitance of 2600 F and a rated voltage of 2.5 V, for temperatures between -20 and 60 °C and for voltages between 0 and 2.5 V. The cell impedances have been measured with a Zahner IM6 Impedance Spectrometer. The supercapacitor is polarized with a dc voltage. A small voltage ripple, typically 10 mV, is superimposed on the dc component. The ripple frequency is swept between 1 mHz and 10 kHz. The measurement of the current amplitude and phase with respect to the injected voltage permits the determination of the real and imaginary part of the impedance as a function of the frequency [8]. The measurements have been performed in a controlled climatic chamber.

3. Capacitance and real part analysis

3.1. Impedance real part

The experimentally determined real component of impedance is plotted as a function of frequency in Fig. 2. As a first approximation, the experimental data shown in this figure can be interpreted in terms of a variable RLC circuit in parallel with a variable leakage resistance. The dependence of resistance on frequency can be divided into four distinct frequency zones as shown in Fig. 2:

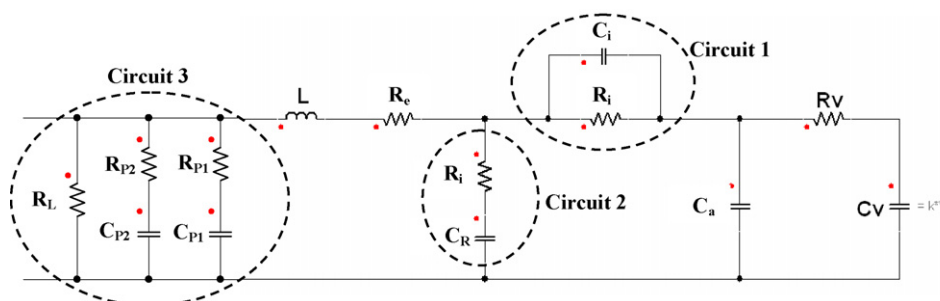


Fig. 1. Supercapacitor equivalent electric model.

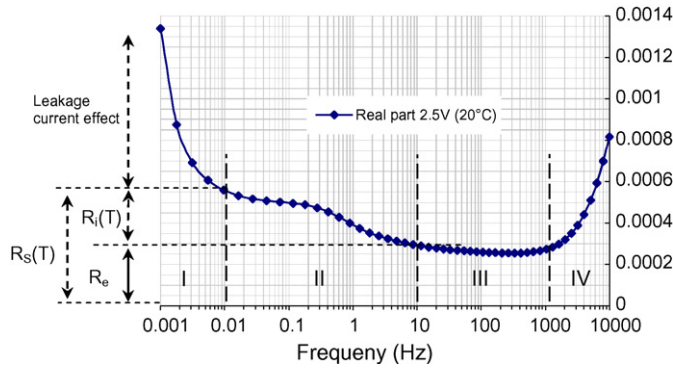


Fig. 2. Impedance real part as a function of frequency with a bias voltage of 2.5 V and a temperature of 20 °C.

- (a) Zone I between 1 and 10 mHz, with characteristic time constant from 10 to 1000 s, is driven by the series and the parallel resistance. This latter is due to the electronic leakage current through the separator, to the charge redistribution inside the electrode and to self-discharge. At very low frequency the parallel resistance contribution is dominating. If the measurement occurs after a very long period of polarization, the resistance amplitude will be much smaller because of the saturation of the leakage current.
- (b) Zone II between 10 mHz and 10 Hz gives the information on the series resistance which is due to the electronic resistance in the conductors R_e and to the ionic resistance in the electrolyte $R_i(T)$ [9]. In this frequency range, the parallel resistance is negligible and the equivalent series resistance (ESR), also called dc resistance, is given by $R_s(T) = R_e + R_i(T)$. The ESR variation is due to the frequency dependency of $R_i(T)$. At low frequency the ions are able to reach electrode area deeper in the activated carbon pores, with the consequence of a longer path for the ions in the electrolyte.
- (c) Zone III between 10 Hz and 1 kHz shows mainly the electronic resistance R_e due to all the connections, particularly the measurement connections, the contact resistance between the activated carbon and the current collector as well as the minimal resistance of the electrolyte [10,11]. Supercapacitor manufacturers generally specify the high frequency ac series resistance at 1 kHz.
- (d) Zone IV between 1 and 10 kHz is due to the supercapacitor inductance and the parasitic inductance of the all connecting cables.

3.2. Impedance imaginary part

The curve of Fig. 3 represents the imaginary part measured by EIS. The dc bias voltage is fixed at 2.5 V and the temperature at 20 °C. The resonance frequency is found around 60 Hz. Above this frequency the supercapacitor behaviour is inductive.

A supercapacitor equivalent inductance of 25 nH can be determined in the high frequency range with the following relation: $L \approx \text{Im}(Z)/2\pi f$.

It is possible to determine the supercapacitor resonance capacitance C_R value of the model at the resonance frequency

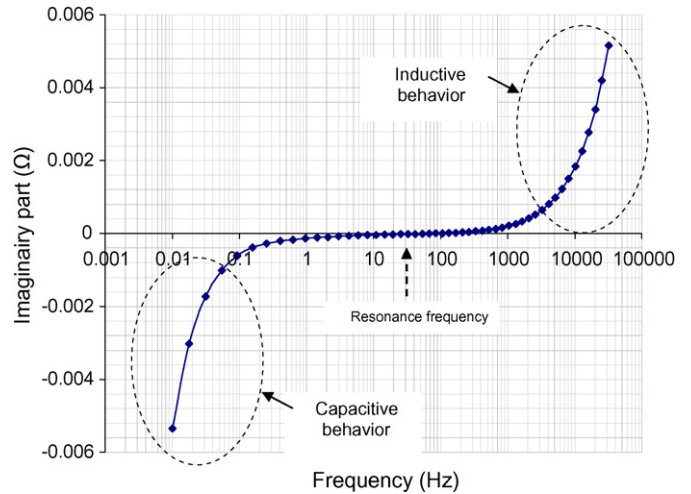


Fig. 3. BCAP0010 impedance imaginary part with a bias voltage of 2.5 V and a temperature of 20 °C.

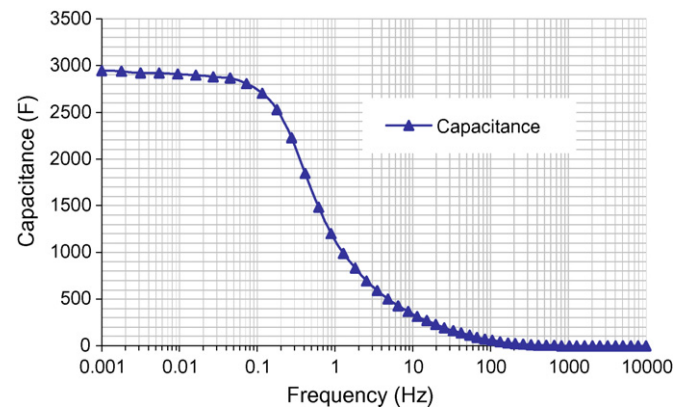


Fig. 4. Differential capacitance frequency dependence with a bias voltage of 2.5 V and a temperature of 20 °C.

with the following relation: $C_R = 1/(2\pi f)^2 L$. For the BCAP0010 the value is in order of 260 F.

Fig. 4 shows the frequency dependence of the supercapacitor capacitance. Once the inductance has been determined, the supercapacitor capacitance can be deduced by using the following expression: $C = 1/2\pi f(2\pi fL - \text{Im}(Z))$, where f is the frequency and L is the inductance. At low frequency ($f < 1$ Hz), the inductance effect is negligible and the capacitance may be estimated with the simplified expression: $C = -1/2\pi f \text{Im}(Z)$.

The capacitance is maximum at low frequency ($f < 0.1$ Hz) because the ions have the time to reach the electrode surface which is hidden deep in the carbon pores. As the frequency increases, the ions cannot follow the applied electric field anymore and do not reach the depth of the electrode pores. To improve the ion dynamic the manufacturers try to optimize the ion access to the pores with particular activation process.

4. Voltage dependence

The supercapacitor capacitance variation due to the voltage finds its origin in the physical structure of the supercapacitor. The capacitance is composed by the series connection of the

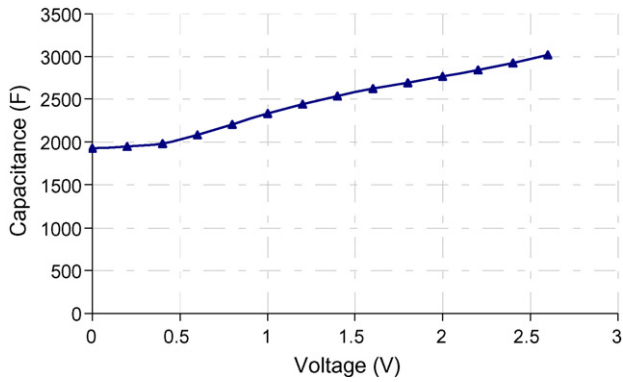


Fig. 5. Differential capacitance as a function of voltage at 20 °C and 1 mHz.

capacitance of each electrode. One possible explanation for the increase in capacitance with voltage can be due to the electrolyte dielectric constant increase, or, to the reduction of the distance separating the charges at the electrode/electrolyte interface. Another explanation is to consider the series connected capacitance, inside the electrode, due to the space charge created by the displacement of charges in the conductor [12]. This charge displacement is at the origin of an electronic capacitance that increases with the density of the electronic states (DOS). Indeed, some of the applied potential extends into the carbon and a space-charge capacitance develops. So, the electrode capacitance may be represented by the series connection of different contributions:

- The capacitance due to the space charge into the carbon.
- The Helmholtz layer capacitance.
- The diffuse capacitance (Gouy, Stern + Chapman).

And in parallel a pseudocapacitance due to functional groups on the surface, in particular [CO]-based one.

Hahn and co-workers have explained some of the behaviour of carbon in detail [13,14]. They have noted that the magnitude of both the capacitance and the conductivity can be directly related to the density of electronic states.

In conclusion, it can be noted that:

- Today almost all electrical engineers involved in the field of supercapacitor fail to take into account the voltage dependence of capacitance in sizing devices to applications.
- Linear dependence of capacitance on voltage is an approximation which improves the modelization precision by 10% compared to constant capacitance approximation.
- The model is valid for more than just the Maxwell technology.

The supercapacitor capacitance may be defined by the ratio: $C = Q/U$, where Q is the charge [15].

Experimental data measured at low frequency (Figs. 5 and 6) shows that the capacitance C increases with the applied voltage within the specified voltage range. To take into account this variation, the capacitance may be approximated with enough accuracy by the sum of a constant contribution C_0 and a linear

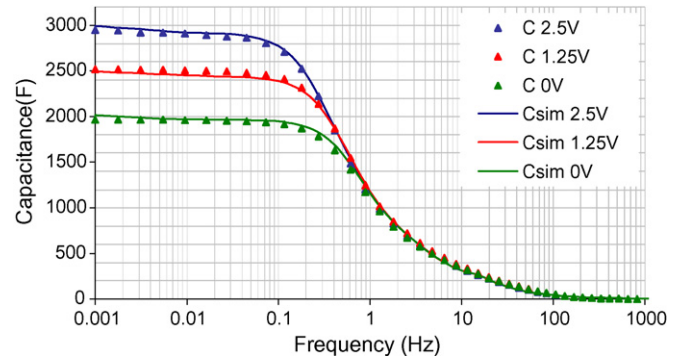


Fig. 6. Measurement and simulation of differential capacitance dependence for bias voltages of 0, 1.25 and 2.5 V and a temperature of 20 °C.

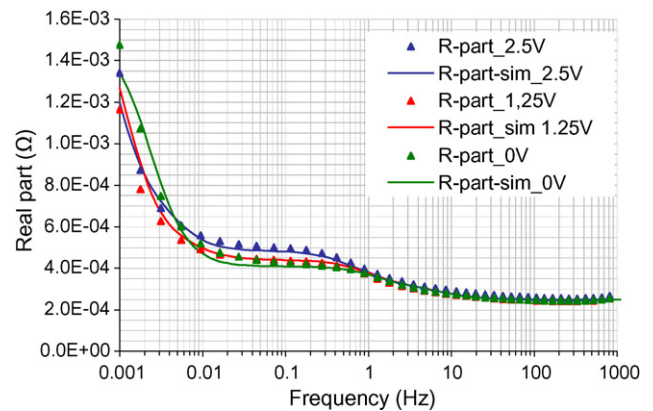


Fig. 7. Measurement and simulation of the impedance real part frequency dependence for bias voltages of 0, 1.25 and 2.5 V and a temperature of 20 °C.

voltage dependent one $C_v = K_v U$, where K_v is a constant. The total capacitance is given by $C = C_0 + C_v$.

The relation between the current and the charge always remains given by: $i = dQ/dt$.

Substituting the Q expression as a function of U and C , taking into account the indirect dependence of C with the time, it is easy to show that the current may be given by: $i(t) = (C_0 + 2K_v U)(dU/dt)$.

By analogy, one may define the differential supercapacitor capacitance as: $C_{diff} = C_0 + 2K_v U$.

In Fig. 5 is plotted the differential capacitance evolution as a function of the supercapacitor voltage. These experimental results show that the capacitance is not linear with the voltage. However, this curve can be considered as linear when the supercapacitor is used between its 2.5 V nominal voltage and the half of this voltage. Hence, in this voltage range, supercapacitor provides 75% of the stored energy.

Fig. 7 represents the real part as a function of the frequency for different voltages. It shows that a higher voltage polarization increases the ESR slightly in the low frequency domain.

5. Thermal dependence

To use supercapacitor in hybrid vehicle applications, it's necessary to study its thermal behaviour. The aim is to establish a supercapacitor model (Fig. 1), which takes into account ther-

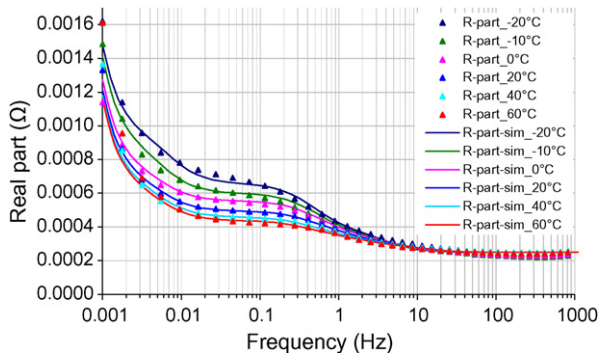


Fig. 8. Measurement and simulation of equivalent resistance frequency dependence for different temperatures for a fixed bias voltage of 2.5 V.

mal variation. The model parameters determination is based on the experimental results obtained by EIS. Fig. 8 represents the real part evolution as a function of supercapacitor temperature for different frequencies. It shows that in high frequency range ($f > 10$ Hz), the series resistance variation with temperature can be neglected. In low frequency range, the equivalent series resistance increases when the temperature decreases. This is due to the fact that the electrolyte ionic resistance R_i is strongly influenced by the temperature. Above 0°C R_i varies slowly with the temperature. Below 0°C the temperature dependence is more important. It is due to the viscosity of the electrolyte that increases in low temperatures what increases the resistance of the electrolyte [16,17].

In the case of the capacitance, the experimental results and the simulations are plotted in Fig. 9. At the first it's important to note the good correlation between experimental and simulation results. At very low frequencies ($f < 0.1$ Hz), the capacitance is almost constant with temperature. It means that the ions penetrate in the depth of the pores of the electrodes regardless of the temperature and there is therefore the same contribution to the capacitance of the double layer for the low temperatures as for higher temperature. In the middle frequency range [0.1, 10 Hz] the capacitance is smaller for low temperature. The reason is the shift of the cut off frequency due to the reduced ion mobility, or in other words to the increase of the series resistance $R_i(T)$.

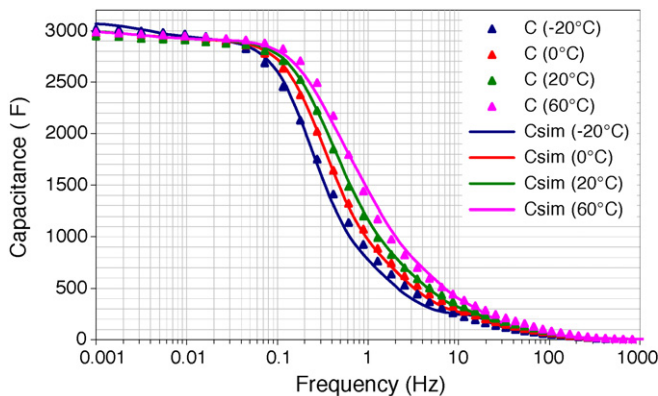


Fig. 9. Measurement and simulation of differential capacitance frequency dependence for different temperatures for a fixed bias voltage of 2.5 V.

6. Determination of model parameters

The model is based on the Zubieta supercapacitor equivalent electric circuit [18], which gives a description of the voltage dependence at low frequency. This behavior may be modeled with an $R_V C_V$ circuit. C_V increases linearly with the voltage by the relation: $C = C_0 + K_V U$.

$C_V = K_V U$, the constant K_V is determined using experimental data (Fig. 5).

C_0 is the voltage constant part capacitance of the supercapacitor cell. In the model it is composed of C_a and C_R , $C_0 = C_a + C_R$. For the BCAP0010 the measurements have shown that the C_a value is in order of 2/3 of the nominal capacitance value provided by the manufacturer.

R_V is a constant resistance it is placed in series with $C_V = K_V U$. The $R_V C_V$ is active only in the low frequency range because it is placed upstream of the principal capacitance, C_a . In practice R_V equals the dc series resistance as explained previously $R_V = R_s(T = 20^\circ\text{C})$.

“Circuit 1” in Fig. 1 has been introduced in the model to take into account the electrolyte ionic resistance temperature dependence in the low frequency range. The parallel capacitance C_i has been used to cancel the contribution of $R_i(T)$ in the high frequency range. For low frequency, the circuit 1 behavior is close to that of resistance $R_i(T)$.

A relationship between R_i and the temperature has been established from experimental results by using EIS. It is given by the following expression: $R_i(T) = R_{20}(1 + \exp(-k_T(T - T_{20}))/2)$, where R_{20} is the electrolyte resistance part $R_i(T)$ at 20°C , T the ambient temperature and k_T is the temperature coefficient $k_T = 0.025^\circ\text{C}^{-1}$.

To have more precision on the model, “ $R_i C_R$ ” of “circuit 2” of Fig. 1 is introduced to increase the value of the capacitance for the average frequencies. Their behaviour is the one of a phase shifter. The example of Fig. 10 represents the equivalent capacity of the model suggested and illustrates the utility of circuit 2 in the model.

“Circuit 3” of Fig. 1 describes the leakage current and the internal charge redistribution. The self-discharge behaviour of supercapacitors is an important factor because it determines the duration time of stored energy on open circuit. For the supercapacitor technology with activated carbon and organic electrolyte, the self-discharge is based on two mechanisms. The first is

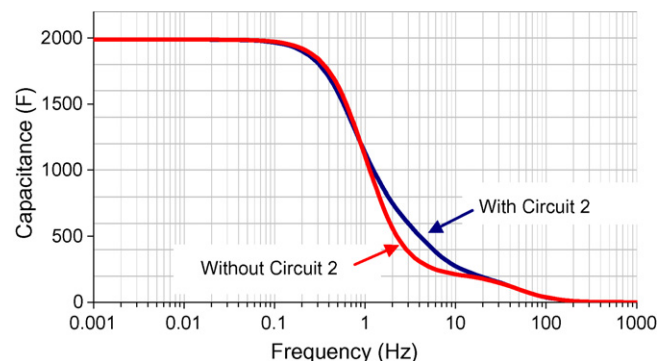


Fig. 10. Simulations using models with and without circuit 2.

due to the diffusion of the excess ionic charges at the interface between the electrode and the electrolyte. The second is due to the impurities in the supercapacitor materials. The supercapacitor self-discharge is also a function of the temperature. Hence, the supercapacitor self-discharge cannot be represented by a simple single resistance. It is necessary to use two different time constant circuits RC , formed, respectively, by the elements $R_{P1}C_{P1}$ and $R_{P2}C_{P2}$ which depend on the voltage and on the operating temperature. It also includes a parallel R_L resistance, which gives the long time leakage current contribution.

In the case of a BCAP0010, the following parameters were determined from experimental results: $R_L = 250 \Omega$, $R_{P2} = (1.2 + 1.12U)$ and $C_{P2} = (55 + 4U)$.

In the case of temperature above 0°C , the experimental results show that:

- C_{P1} depends only on the voltage: $C_{P1} = k_1U$, with $k_1 = 26 [\text{F V}^{-1}]$.
- R_{P1} is constant and is equal to $R_{P1} = 0.6 \Omega$.

In the case of temperature below 0°C :

- C_{P1} depends on the temperature and the voltage with the following relation: $C_{P1} = (26 - 1.6T)U$.
- R_{P1} depends on the temperature $R_{P1} = (0.6 + (T/60))$.

The effect of the temperature on the capacitance C_i is negligible. The latter strongly depends on the frequency of use starting from 15 Hz.

For a frequency lower than 15 Hz, C_i is constant and its value is in order of 260 F. When the frequency is higher than 15 Hz, this capacitance is given as following: $C_i = 15 \times 260/f$. In the following, simulation results are obtained using the model presented in Fig. 1.

7. Model validation

The model proposed in Fig. 1 allows describing the supercapacitor behaviour in the full frequency range and takes into account supercapacitor voltage and temperature variations.

The total differential capacitance found in the low frequency range is given by:

$$C_{\text{diff}} = C_a + C_R + C_{P1} + C_{P2} + 2K_VU$$

where K_V is the linear coefficient and is equal to $K_V = 195 \text{ F V}^{-1}$ for a BCAP0010.

7.1. Validation with the electrochemical impedance spectroscopy

A complete analysis of the results allows establishing a model of supercapacitor taking into account the frequency, the voltage and the temperature of the device. A simulation of the model in the frequency domain has been achieved in order to compare the simulation results with the experimental ones. Figs. 6 and 7 represent, respectively, the evolution of the capacitance and the impedance real part according to the frequency for bias voltages

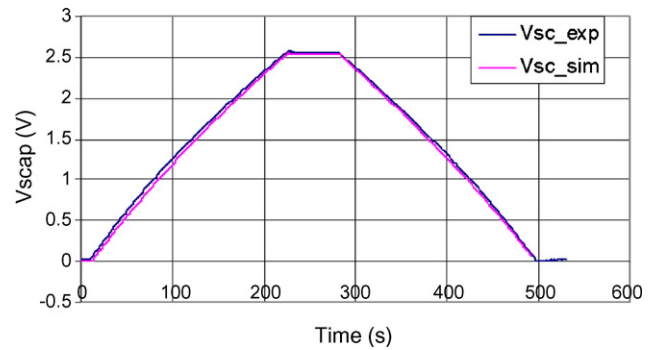


Fig. 11. Simulation and experimental results for a 2600 F supercapacitor with a constant 30 A charge/discharge as a function of time.

of 0, 1.25 and 2.5 V and a temperature of 20°C . These results show the good agreement between the experimental result and the simulation ones.

In order to validate the proposed model which takes into account the supercapacitor temperature variations, supercapacitor real part and capacitance are plotted, for different temperatures, respectively, in Figs. 8 and 9.

It's clear to see the good correlation between simulations results with the proposed model and experimental ones.

7.2. Supercapacitor charge/discharge at constant current validation

To validate the proposed model in dc regime, a comparison between the simulation and the experimental results was realized. Fig. 11 shows the experimental results and the simulation ones. Supercapacitor is charged and discharged at constant current (in order of 30 A). These results show the good correlation between the experimental and the simulation data.

Another comparison between experimental results and simulation ones has been realized. Fig. 12 represents this application where supercapacitor is discharged by using an active load controlled by an external voltage. The supercapacitor is discharged with a square signal current. This last varies between 0 and 60 A with 50 mHz of frequency, the duty cycle is 0.5.

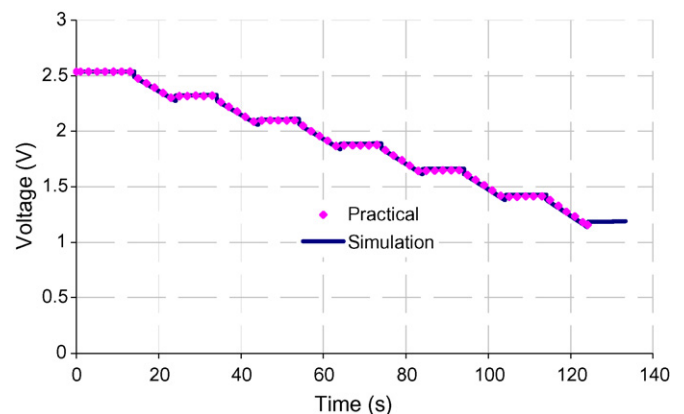


Fig. 12. Two thousand six hundred farad supercapacitor discharge with a 50 mHz square current with amplitude level of 0 and 60 A.

Table 2
Model parameters for a BCAP0010 supercapacitor

Parameters	Values
L	25 nH
R_c	0.25 m Ω
R_{20}	0.22 m Ω
R_v	0.5 m Ω
C_R	260 F
C_a	1700 F
K_v	195 F V ⁻¹
R_L	250 Ω

These results show the good agreement between simulation and experiment.

Table 2 is a summary of all the model parameters necessary to describe BCAP0010 behaviour as a function of the frequency, the voltage and the temperature.

8. Conclusion

This paper presents an equivalent electrical circuit for Maxwell 2600 F supercapacitor model. The originality of this study is in the fact that the established model takes into account frequency, voltage and temperature variations of the device and its environment. The electric equivalent circuit proposed will be easy to use in several analog simulators. It is well adapted to some studies concerning behavior of supercapacitors when used in automotive applications thanks to sensitivity analysis induced by thermal, frequency and voltage parameters. The simulation results are in good agreement with the experimental ones.

The proposed model is based on only 14 devices. The correlation has been verified in the frequency domain with an impedance spectrometer and with supercapacitor charge/discharge at constant current. In the frequency domain the results have been verified in the temperature range between –20 and 60 °C and in the voltage range between 0 and 2.5 V.

References

- [1] B.E. Conway, *Electrochemical Supercapacitors: Scientific Fundamentals and Technological Applications*, Kluwer Academic Press/Plenum Publishers, New York, 1999, pp. 377–556.
- [2] A. Burke, *J. Power Sources* 91 (2000) 37–50.
- [3] B.E. Conway, W.G. Pell, *J. Power Sources* 105 (2002) 169–181.
- [4] R. De Levie, in: P. Delahay (Ed.), *Advances in Electrochemistry and Electrochemical Engineering*, vol. 6, Wiley, New York, 1967, pp. 329–397.
- [5] F. Belhachemi, S. Raël, B. Davat, *Proceedings of the Industry Applications Conference, 2000. Conference Record of the 2000 IEEE*, vol. 5, GREEN-INPL-CNRS (UPRE), October 8–12, 2000.
- [6] E. Karden, S. Buller, R.W. De Doncker, *Electrochim. Acta* 47 (2002) 2347–2356.
- [7] D. Qu, H. Shi, *J. Power Sources* 74 (1998) 99–107.
- [8] S. Buller, E. Karden, D. Kok, R.W. De doncker, *IEEE Trans. Ind. Appl.* 38 (6) (2002) 1622–1626.
- [9] A. Chu, P. Braatz, *Comparison of Commercial Supercapacitors and High-power Lithium-ion Batteries for Power-assist Applications in Hybrid Electric Vehicles. I. Initial Characterization* (June 2002), HRL Laboratories, LLC 3011, Malibu Canyon Road, Malibu, CA 90265-4797, USA, 2002.
- [10] R. Kötz, M. Carlen, *Electrochim. Acta* 45 (2000) 2483–2498.
- [11] C. Portet, P.L. Taberna, P. Simon, C. Laberty-Robert, *Modification of Al Current Collector Surface by sol-gel Deposit for Carbon-Carbon Supercapacitor Applications*, CIRIMAT, UMR CNRS 5085, 118 Route de Narbonne, Toulouse Cedex 31062, France.
- [12] A.G. Pandolfio, A.F. Hollenkamp, *J. Power Sources* 157 (2006) 11–27.
- [13] M. Hahn, M. Baertschi, O. Barbieri, J.-C. Sauter, R. Kötz, R. Gallay, *Electrochem. Solid State Lett.* 7 (2) (2004) A33–A36.
- [14] R. Kötz, M. Hahn, M. Baertschi, O. Barbieri, J.-C. Sauter, R. Gallay, *Proceedings of the 13 International Seminar on Double Layer Capacitor and Similar Energy Storage Devices*, Deerfield Beach, Floride, December 8–10, 2003.
- [15] V. Hermann, A. Schneuwly, R. Gallay, *Proceedings of the PCIM, Nürnberg*, 2001.
- [16] W. Lajnef, O. Briat, S. Azzopardi, E. Woïrgard, J.-M. Vinassa, *Ultracapacitors Electrical Modelling Using Temperature Dependent Parameters*, ESSCAP BELFORT, 2004.
- [17] H. Gualous, D. Bouquain, A. Berthon, J.M. Kauffmann, *J. Power Sources* 123 (2003) 86–93.
- [18] L. Zubieta, R. Bonert, *Proceedings of the IEEE-IAS'98*, 1998, pp. 1149–1154.